deltaic environment of the Mazon Creek marine-brackish assemblage. Alternatively, *Myxinikela* may be an adult and characteristics of the living myxines might have evolved phylogenetically later. Thus *Myxinikela* is primitive relative to living myxiniforms in the above features as well as the larger eyes. Finally, in the last 30 years of intense collecting efforts, only one hagfish but in excess of 40 lampreys have been found. Perhaps hagfish were rare entrants to the Mazon Creek habitat.

REFERENCES AND NOTES

1. P. Forey, *J. Vert. Paleontol.* **4**, 330 (1984); J. G. Maisey, *Cladistics* **2**, 201 (1986); P. Janvier, *J. Vert. Paleontol.* **1**, 121 (1981).
2. E. Stensio, in *Traité de Zoologie*, P. P. Grassé, Ed. (Masson, Paris, 1958), vol. 13, pp. 173–425.
3. D. Bardack and R. Zangerl, *Science* **162**, 1265 (1968).
4. P. Janvier and R. Lund, *J. Vert. Paleontol.* **2**, 407 (1983).
4a. The holotype and single specimen belongs to Northeastern Illinois University (NEIU), Department of Earth Sciences (MCP 126) and came from SE 1/4, SE 1/4, Sec. 29, T. 32N, R. 9E.
5. G. Baird, C. W. Shabica, J. C. Anderson, E. S. Richardson, Jr., *J. Paleontol.* **59**, 253 (1985).
6. W. Marinelli, in *Vergleichende Anatomie und Morphologie der Wirbeltiere*, W. Marinelli and A. Strenger, Eds. (Deuticke, Vienna, 1956), part 2.
7. F. J. Cole, *Trans. R. Soc. Edinb.* **41**, 749 (1905).
8. M. W. Hardisty, in *The Biology of Lampreys*, M. W. Hardisty and I. V. Potter, Eds. (Academic Press, London, 1982), pp. 165–259.
9. B. K. Fernholm and K. Holmberg, *Vision Res.* **15**, 253 (1974).
10. L. Neumayer, *Arch. Ital. Anat. Embrio. Suppl.* **40**, 1 (1938).
11. H-P. Schultze and D. Bardack, *J. Vert. Paleontol.* **7**, 1 (1987).

12. I thank D. Siroka and S. Siroka for the opportunity to study the specimen, J. Weinstein of the Field Museum of Natural History for the photographs, and R. Rosenblatt for the loan of a cleared-stained specimen of *Eptatretus*.

15 May 1991; accepted 7 August 1991

Calcium Gradients Underlying Polarization and Chemotaxis of Eosinophils

RODNEY A. BRUNDAGE, KEVIN E. FOGARTY, RICHARD A. TUFT, FREDRIC S. FAY

The concentration of intracellular free calcium ($[Ca^{2+}]_i$) in polarized eosinophils was imaged during chemotaxis by monitoring fluorescence of the calcium-sensitive dye Fura-2 with a modified digital imaging microscope. Chemotactic stimuli caused $[Ca^{2+}]_i$ to increase in a nonuniform manner that was related to cell activity. In cells moving persistently in one direction, $[Ca^{2+}]_i$ was highest at the rear and lowest at the front of the cell. Before cells turned, $[Ca^{2+}]_i$ transiently increased. The region of the cell that became the new leading edge had the lowest $[Ca^{2+}]_i$. These changes in $[Ca^{2+}]_i$ provide a basis for understanding the organization and local activity of cytoskeletal proteins thought to underlie the directed migration of many cells.

THE ABILITY OF CELLS TO MIGRATE toward a directional stimulus is a basic property of virtually all cells at some stage in their development (*1*) Directed migration results from the development of a polarized cell morphology (*2*). The region of the cell closest to the attractant forms a broad lamellipod whose leading edge then moves toward the stimulus. The posterior contents of the cell flow forward into this lamellipod and the rearmost regions become constricted. These local differences must reflect local differences in cell chemistry, but these chemical processes are not well understood. Many stimuli that induce polarization and chemotaxis also cause $[Ca^{2+}]_i$ to rise, and where a rise in $[Ca^{2+}]_i$ has been noted (*3*), it has often (*4*), but not always (*5*), been spatially nonuniform in nature. The relation between the $[Ca^{2+}]_i$ signal and local changes in cell behavior has been difficult to understand, and the spatial patterns observed have been variable (*6*) perhaps because of local differences in indicator distribution in the cytoplasm or into cellular compartments (*7*). Furthermore, the optical conditions required for assessing $[Ca^{2+}]_i$ often did not allow for simultaneous assessment of cell morphology and behavior. We have now observed changes in $[Ca^{2+}]_i$ during polarization and chemotaxis by simultaneously imaging both $[Ca^{2+}]_i$ and cell morphology under conditions obviating many of these problems. Single eosinophils from the newt *Taricha granulosa* were studied because of their large size and rapid responsiveness to chemotactic stimuli (*8*).

Experiments were carried out to determine if treatments with agents that interfere with Ca^{2+} signaling altered the ability of eosinophils to polarize and move in response to newt serum. Exposure to newt serum (10%) induces polarization, chemokinesis, and chemotaxis in these cells (*8*). Treatment with agents that block Ca^{2+} entry into cells (EGTA, a chelator of extracellular Ca^{2+}; verapamil, an organic Ca^{2+} channel antagonist; and Co^{2+}, an inorganic Ca^{2+} channel blocker), caused the cells to round up and inhibited their movement (*9*). Caffeine, which releases Ca^{2+} from internal stores and prevents regulation of cytoplasmic Ca^{2+}, had similar effects as did the Ca^{2+}-specific ionophore ionomycin (*9*). Ionomycin exerted these inhibitory effects at both normal (1.8 mM) and reduced (1 μM) extracellular $[Ca^{2+}]$. By contrast, the K^+-specific ionophore, valinomycin (0.6 μM) had no effect on cell movement or shape at both normal (3 mM) and elevated (120 mM) concentrations of extracellular K^+ (*10*). This suggests that the membrane potential of the cell is unimportant for polarization and locomotion in response to serum and that the effects of ionomycin are specific to its ability to act as a Ca^{2+} ionophore. These treatments had the expected effect on $[Ca^{2+}]_i$; for example, treatment of cells with verapamil lowered $[Ca^{2+}]_i$ by 24.7 ± 11.1% in three cells, ionomycin increased $[Ca^{2+}]_i$ by 801 ± 233% in five cells, and caffeine reduced $[Ca^{2+}]$ in regions believed to reflect Ca^{2+} in internal stores (*10*). Thus, agents expected to lower $[Ca^{2+}]_i$ diminished polarity and locomotion as did agents that raised $[Ca^{2+}]_i$. Regulation of $[Ca^{2+}]_i$ therefore appeared to be necessary for these processes, suggesting that Ca^{2+} functions in chemoattractant signal transduction.

We therefore investigated the relation between cell shape, cell movement, and $[Ca^{2+}]_i$. $[Ca^{2+}]_i$ was measured with the Ca^{2+}-sensitive fluorescent probe Fura-2, which was microinjected into the cells in the free acid form to obviate problems from incomplete de-esterification or intracellular compartmentation that may occur when cells are incubated with the acetoxymethyl ester of this dye (*11*). Pairs of fluorescent images at 340 and 380 nm excitation were taken in rapid succession with a high efficiency, low noise, cooled, charge-coupled device (CCD camera) at intervals of 10 to 30 s, while phase contrast images were recorded at more frequent intervals at 680 nm (Fig. 1A).

Eosinophils stimulated with serum developed a polarized motile morphology (Fig. 1B) and increased their overall $[Ca^{2+}]_i$. The average $[Ca^{2+}]_i$ in resting

Department of Physiology, Biomedical Imaging Group Program in Molecular Medicine, University of Massachusetts Medical School, Worcester, MA 01605.

cells was 76.9 ± 5.3 nM. When these same cells had polarized in response to serum, $[Ca^{2+}]_i$ increased to 122.9 ± 8.2 nM. In the polarized moving eosinophil, $[Ca^{2+}]_i$ appeared to be non-uniform, unlike that in unstimulated nonpolarized cells, and in addition $[Ca^{2+}]_i$ varied over a greater range (23 nM) over the same time period (15 min) in polarized moving cells than in resting cells (12 nM).

To determine if the spatial heterogeneity and fluctuations of $[Ca^{2+}]_i$ in stimulated cells were related to the direction of polarization or movement or both, cells were imaged as they migrated and spontaneously changed direction in medium containing serum (10%). During periods when the cell maintained a given direction of polarization and movement, a shallow but clearly detectable gradient of $[Ca^{2+}]_i$ existed with $[Ca^{2+}]_i$ at the front of the cell lower than that at the rear (Fig. 2). When the cell was changing direction, cytoplasmic $[Ca^{2+}]_i$ was higher on average but a gradient was still seen; the new leading lamellipod had the lowest $[Ca^{2+}]_i$. This pattern was consistently observed in a total of 70 images of five cells migrating in response to serum. A statistically significant ($P < 0.005$) decreasing gradient of $[Ca^{2+}]_i$ from the rear to the front of cells was characteristic of both turning cells and cells moving consistently in one direction (Fig. 3) (*12*). The average $[Ca^{2+}]_i$ in the whole cell was 2.6 ± 0.1 (SD) times higher during a turn than in the same five cells moving straight ahead. A similar gradient of $[Ca^{2+}]_i$ was observed in cells migrating toward a micropipette from which serum (10%) was slowly being ejected into serum-free medium. Under these conditions, the average $[Ca^{2+}]_i$ was 0.77 ± 0.02 (SD) times that in the same three cells when they were migrating in medium containing a uniform concentration of serum; the gradient of $[Ca^{2+}]_i$ was also less steep. The average velocity of these cells when moving straight toward the pipette was lower (5.4 ± 1.4 μm/min) than when these same cells were moving persistently in one direction in the presence of serum (10%) (11.4 ± 3.9 μm/min).

Although the nonuniformity of the $[Ca^{2+}]_i$ images might reflect nonuniformity in the dye distribution between cytoplasm and intracellular compartments, this is unlikely as the injected Fura-2 appears to be free in the cytoplasm; more than 98.5% of it rapidly ($t < 2.75$ min) left cells permeabilized with digitonin (50 μM) (*13*). Nor does the observed gradient of $[Ca^{2+}]_i$ reflect the admixture of a high nuclear $[Ca^{2+}]$ at the rear of the cell with a lower cytoplasmic $[Ca^{2+}]$ signal; a similar $[Ca^{2+}]$ gradient (0.92 ± 0.18 nM/μm) was observed in the posterior region occupied by the nucleus and in anterior regions beyond the nucleus (0.95 ± 0.16 nM/μm) in the three cells analyzed. Although Fura-2 fluorescence is sensitive to viscosity (*14*), the apparent gradient of $[Ca^{2+}]_i$ is not due to a possible gradient of microviscosity resulting from regional differences in cytoplasmic organization in polarized cells (*15*). Measurements of the fluorescence anisotropy of Fura-2, both in solution and in eosinophils, indicated that observed differences in $[Ca^{2+}]_i$ could not be explained by the effects of viscosity on Fura-2 (*16*). Thus, the differences in local $[Ca^{2+}]_i$ that have been calculated from images of Fura-2 fluorescence in polarized and locomoting cells appear to reflect genuine gradients of $[Ca^{2+}]_i$ within these cells.

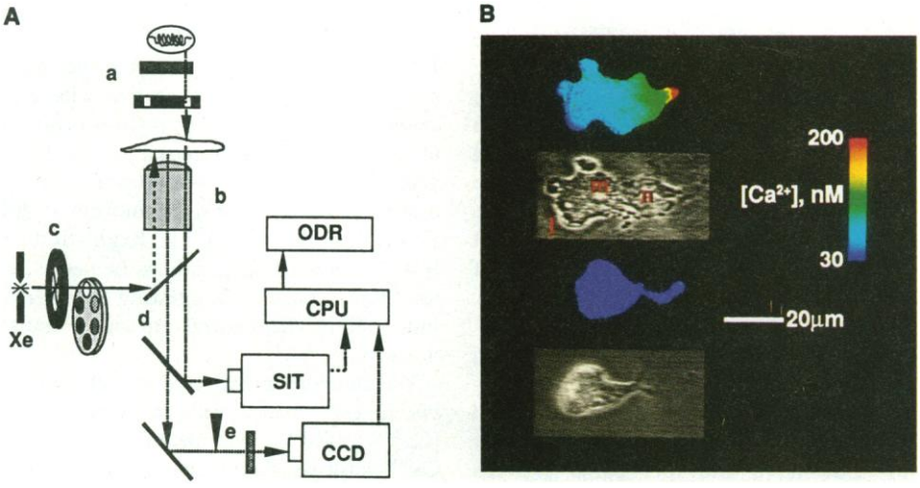

Fig. 1. Simultaneous measurement of $[Ca^{2+}]_i$ with Fura-2 and cell morphology with phase contrast optics. (**A**) Schematic illustration of digital imaging microscope. (a) Phase illumination, filtered to 680-nm central wavelength. (b) Nikon UVF 40× Phase 4 objective. (c) Xe arc, shutter and filter wheel (AZI Corp., Dedham, Massachusetts). (d) Dichroic mirrors: upper-long pass, 50% transmission at 430 nm, lower-short pass, 50% transmission at 605 nm. (e) Mask to limit image area to 390 by 292 pixels on 390 by 584 pixel CCD detector array. An SIT camera records phase-contrast images and the digitized video is stored on an optical disc recorder (ODR). Fura-2 fluorescence is imaged on the unmasked CCD area by alternately exposing the specimen for 0.5 s with 340- and 380-nm illumination, the 340-nm image stored on the CCD being moved to the masked region during the 100-ms filter changing time. The CPU controls and coordinates filter wheel position, digitized SIT imaging, and the readout to hard disk (~8 s) of the 340- and 380-nm images for storage prior to processing (*26*). (**B**) Phase contrast images and pseudocolored images of $[Ca^{2+}]_i$ in an eosinophil during stimulation with newt serum (10%) (top) and after tenfold dilution of serum (bottom) with amphibian culture medium (ACM). The mean $[Ca^{2+}]_i$ in this cell during serum stimulation was 139 nM and was 72 nM after serum dilution. In the presence of serum, these eosinophils were highly polarized and migrated rapidly (mean velocity = 11.8 ± 1.2 μm/min); when serum was diluted they became more spherical in shape and immobile. In the polarized motile state, they have a lamellipod (*l*) at the rapidly extending leading edge, the nucleus (n) is positioned at the tapered rear of the cell, and the microtubule organizing center (m) is evident as a region near the nucleus devoid of granules that otherwise fill the rest of the cytoplasm.

To determine if the observed gradient of $[Ca^{2+}]_i$ might function in determining the axis of polarization and subsequent direction of locomotion, $[Ca^{2+}]_i$ and phase contrast images were recorded in cells that were induced to change their direction of movement either 90° or 180° by reorienting the gradient of chemoattractant to which they were exposed (Fig. 4). Within 50 s after the gradient of serum was reversed, the gradient of $[Ca^{2+}]_i$ also reversed in the cell (Fig. 4A); at this time, the cell had neither slowed nor reversed its direction of movement, nor had it developed a lamellipod in the new direction of the stimulus. When another cell was induced to make a 90° turn, overall $[Ca^{2+}]_i$ increased and a new gradient of $[Ca^{2+}]_i$ appeared with the lowest $[Ca^{2+}]_i$ in the region which subsequently became the new leading edge of the cell (Fig. 4B). The high sensitivity and low noise of the CCD camera provide images of unusual clarity and accuracy; however, because of the slow read out of this device, wavelength image pairs could be obtained only once every 15 s. Thus, aspects of the Ca^{2+} signal that occurred infrequently or briefly may have escaped detection. Our observations do reveal that $[Ca^{2+}]$ is nonuniformly distributed in a manner related to cell activity and that changes in the direction of motion and the preceding repolarization of cells

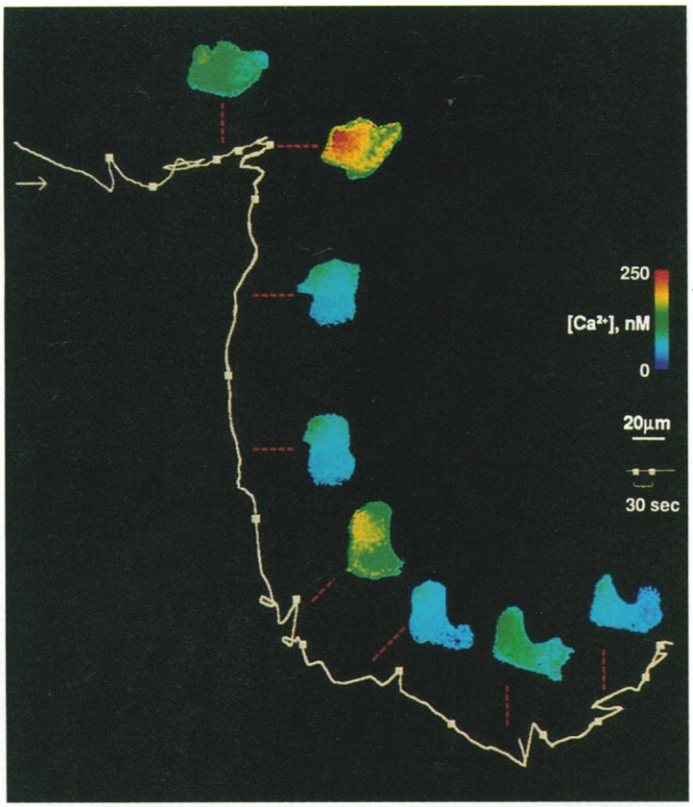

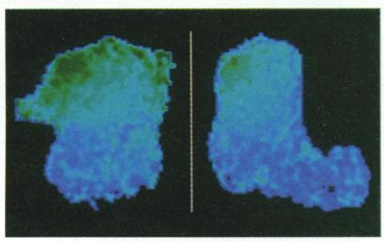

Fig. 2. Pseudocolored images of $[Ca^{2+}]_i$ and the path of motion of an eosinophil in medium containing serum (10%). The path shown is the position of the cell centroid calculated from phase-contrast images at 10-s intervals over a total period of 8.3 min. The initial position of the cell centroid is at the upper left. Selected images of $[Ca^{2+}]_i$ are shown with a red line pointing from the image to the points on the cell centroid trajectory at which the $[Ca^{2+}]_i$ image was obtained. The centroid track has been enlarged 5× relative to the $[Ca^{2+}]_i$ images. As illustrated in the $[Ca^{2+}]_i$ images at the bottom, which have been magnified by an additional 2×, a gradient of decreasing $[Ca^{2+}]_i$ from the back to front of each cell was consistently observed when cells were migrating persistently in a straight course. This gradient may be barely perceptible in the unmagnified $[Ca^{2+}]_i$ images.

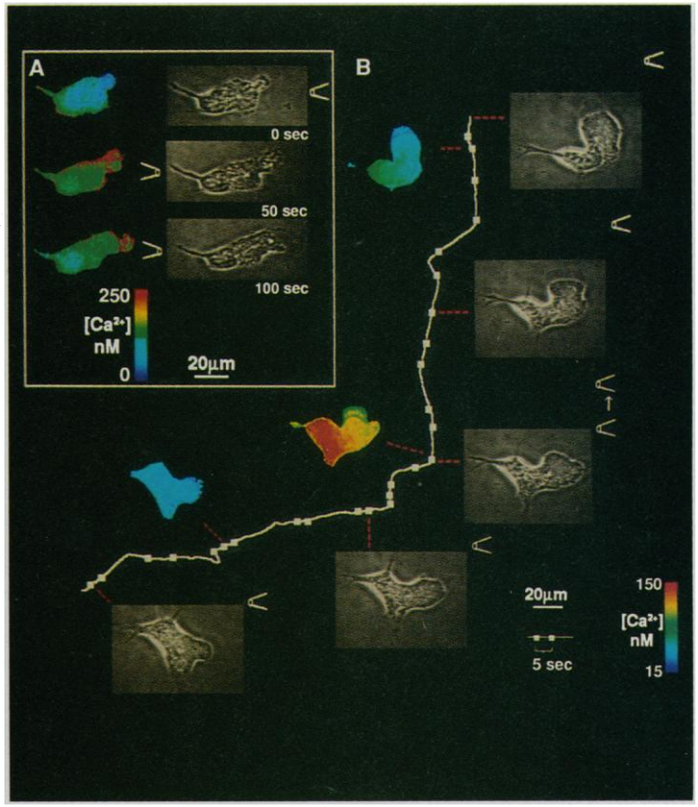

Fig. 4. Phase-contrast and pseudocolored $[Ca^{2+}]_i$ images of two eosinophils migrating toward a pipette from which serum was being ejected. (**A**) Effect of moving the pipette from the front to the rear. The position of the serum-filled pipette is indicated with each $[Ca^{2+}]_i$ image; it was between the first and second $[Ca^{2+}]_i$ images. Phase-contrast images correspond to the points when fluorescent Fura-2 images were taken. (**B**) Effect of moving a pipette from which serum was slowly being ejected from the front to the side of another cell. The long white line indicates the track of the cell centroid, determined from phase-contrast images taken at 5-s intervals as indicated by the white squares. The track has been enlarged 13× relative to the $[Ca^{2+}]$ and phase images. The position of the serum- filled pipette is indicated to the right of each phase contrast image. Five seconds before the second $[Ca^{2+}]$ image was recorded, the pipette was moved to induce the cell to turn, as is indicated by the arrow and the subsequent change of direction of the centroid track.

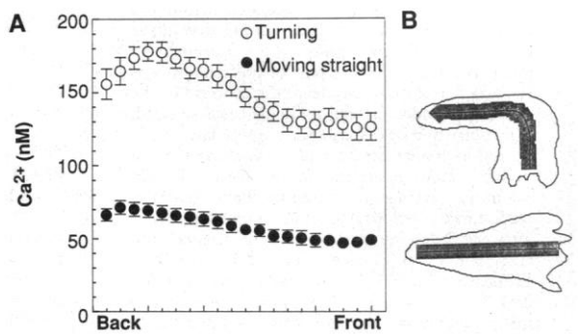

Fig. 3. Variation of $[Ca^{2+}]_i$ along the long axis of five eosinophils during their chemotactic response to serum. (**A**) Relation of $[Ca^{2+}]_i$ to fractional distance from front to back of eosinophils during response to serum. Values shown are means ± SEM for $[Ca^{2+}]_i$ in 16 and 13 images of cells in 10% serum moving straight or turning, respectively. The $[Ca^{2+}]_i$ along the long axis of the cell was calculated as shown in (B). (**B**) Schematic illustration of the method used to extract information from $[Ca^{2+}]_i$ images. A line connecting the center of the leading lamellipod to the center of the uropod was drawn with interactive computer graphics software for cells migrating persistently (>25 s) in one direction in serum (lower panel) or changing their direction of migration in serum (upper panel). Mean values for $[Ca^{2+}]_i$ along this line were calculated from values up to 10 pixels on either side along a normal at each point. To compare $[Ca^{2+}]_i$ gradients in different sized cells, the line was divided into 20 equal segments and the mean $[Ca^{2+}]_i$ for each segment was calculated.

are accompanied by a rise in $[Ca^{2+}]_i$ and reorientation of the $[Ca^{2+}]_i$ gradient. The formation of a new leading lamellipod never preceded the rise in $[Ca^{2+}]_i$ and reorientation of the $[Ca^{2+}]_i$ gradient in 17 images of eight cells and we have seen reorientation of the $[Ca^{2+}]_i$ gradient which definitely preceded any detectable behavioral or structural changes (Fig. 4A). Thus, the results indicate that the $[Ca^{2+}]_i$ gradient may be responsible, at least in part, for inducing a gradient of chemical reactions that underlie chemotaxis.

We might gain insight into the nature of the Ca^{2+}-dependent reactions that link the $[Ca^{2+}]_i$ gradient to the regional specialization of cells during polarization and chemotaxis from earlier hypotheses regarding the role of the cytoskeleton in directed cell locomotion (*17, 20*) and from emerging information regarding the intracellular

distribution and the Ca^{2+} sensitivity of proteins thought to regulate cytoskeletal function. The higher $[Ca^{2+}]_i$ at the rear of the cell should favor myosin II activity in the cortex there, resulting in constriction of the rear and forward propulsion of the cell contents. By contrast, the activity of myosin I, a tailless myosin believed to function in the extension of lamellipods (*18*), should be highest at the front of the cell in that its activity is inhibited with increasing $[Ca^{2+}]_i$ (*19*). Accumulation of these myosins would be expected to occur in their region of highest activity (*20*) if they are free to move within the cell (as myosin II appears to be) (*21*). Finally, the gradient of $[Ca^{2+}]_i$ may act through proteins such as gelsolin that sever actin filaments in a Ca^{2+}-dependent manner (*22*) to produce net assembly and disassembly of actin filaments at the front and rear, respectively; this pattern of actin dynamics has been observed in locomoting polarized cells (*23*). Although the direction of the observed $[Ca^{2+}]_i$ gradient provides a basis for understanding likely regional differences in Ca^{2+}-dependent cytoskeletal processes, the differences in $[Ca^{2+}]_i$ we have detected are small relative to the Ca^{2+} sensitivity for many of these reactions in vitro. However, the Ca^{2+} sensitivity of a multistep pathway may be much greater than the Ca^{2+} binding step (for example, Ca^{2+} binding to calmodulin) if the downstream targets are present at much lower concentrations or have very high affinities for the Ca^{2+}-bound effector. Certainly this is the case for the calmodulin myosin light chain phosphorylation cascade (*24*). The local differences in cytoskeletal activity required for directed migration may be small, especially if regional differences in cytoskeletal activity are self-amplifying because of the movement of the cytoskeletal proteins to regions of highest activity.

Both the steepness of the gradient of $[Ca^{2+}]_i$ and the average $[Ca^{2+}]_i$ were increased in cells changing their direction of migration. The rise in $[Ca^{2+}]_i$ might facilitate (*25*) the remodeling of attachments to the substrate that must accompany a sudden change in the direction of cell motion. The enhanced steepness of the $[Ca^{2+}]_i$ gradient might accelerate the redistribution of myosin isoforms, actin and the consequent remodeling of cell shape. Once the overall shape and molecular distribution have been reestablished, a shallower $[Ca^{2+}]_i$ gradient, and a lower overall $[Ca^{2+}]_i$, may be sufficient to maintain the asymmetry of the cell and drive it forward. The rate of motion of cells, the $[Ca^{2+}]_i$, and the spatial distribution of Ca^{2+} all varied depending on whether cells were stimulated by a gradient or uniform concentration of serum. Thus, the characteristics of the Ca^{2+} signal may influence the rate of cell motion in the steady state as well.

Although this study has focused on local differences in $[Ca^{2+}]_i$ underlying the polarization-chemotactic response, the observed local differences presumably reflect the concentration of other molecules that regulate the changes in $[Ca^{2+}]_i$. The pattern of distribution of these regulating molecules may also contribute to the local control of reactions integral to the polarization-chemotactic response.

REFERENCES AND NOTES

1. J. P. Trinkhaus, *Cells into Organs. The Forces that Shape the Embryo* (Prentice-Hall, Englewood Cliffs, NJ, ed. 2, 1984).
2. S. H. Zigmond, *J. Cell Biol.* **77**, 269 (1978).
3. D. L. Taylor, J. R. Blinks, G. Reynolds, *ibid.* **86**, 599 (1980); T. Pozzan, D. P. Lew, C. B. Wollheim, R. Y. Tsien, *Science* **221**, 1413 (1983); R. Snyderman and E. J. Goetzl, *ibid.* **213**, 830 (1981).
4. D. L. Taylor, J. R. Blinks, G. Reynolds, *J. Cell Biol.* **86**, 599 (1980); D. W. Sawyer, J. A. Sullivan, G. L. Mandell, *Science* **230**, 663 (1985).
5. P. W. Marks and F. R. Maxfield, *J. Cell Biol.* **110**, 43 (1990).
6. D. L. Taylor, J. R. Blinks, G. Reynolds, *ibid.* **86**, 599 (1980); K. Kuroda, Y. Yoshimoto, Y. Hiramoto, *Protoplasma* **144**, 64 (1980); M. Poenie, R. Y. Tsien, A. Schmidt-Verhulst, *EMBO J.* **6**, 2223 (1987); L. S. Gray, J. R. Gnarra, J. A. Sullivan, G. L. Mandell, V. H. Engelhart, *J. Immunol.* **141**, 2424 (1988).
7. E. D. W. Moore, P. L. Becker, K. E. Fogarty, D. A. Williams, F. S. Fay, *Cell Calcium* **11**, 157 (1990).
8. M. P. Koonce, R. A. Cloney, M. W. Berns, *J. Cell Biol.* **98**, 1999 (1984). Chemotaxis in response to a gradient of newt serum (0 to 10%) was demonstrated with a blind well, Boyden type, chemotaxis assay (R. A. Brundage and F. S. Fay, unpublished observations).
9. Agents expected to interfere with Ca^{2+} signaling were added to the medium in which an eosinophil was migrating. Changes in the extent of polarization and rate of movement were calculated from changes in the position and shape of the cell perimeter determined by interactive analysis of phase contrast images recorded for an average of 2.8 min before and 9.2 min after treatment. The rate of cell movement was calculated before and after treatment from the change in position of the centroid between two sets of images collected 40 s apart. An index of the extent of polarization was calculated as the variance from the centroid to the cell edge divided by the mean distance squared. This polarity index is zero for a nonpolarized cell having a circular profile and increases as the cell becomes more polarized and asymmetric. Within 3.5 min on average the maximum change in polarization index (polarity) and rate of motion (speed) after the following treatments were: *Control*: polarity = 8.8 ± 0.8, speed = 11.8 ± 1.2 (n = 23); EGTA (5 m*M*; $[Ca^{2+}]$ = 50 nM): polarity = 5.2 ± 1.7, speed = 3.7 ± 1.1 (n = 6); *Cobalt* (10 mM): polarity = 1.0 ± 0.7, speed = 1.3 ± 0.3 (n = 5); *Verapamil* (50 μM): polarity = 4.5 ± 0.5, speed = 4.4 ± 0.6 (n = 5); *Caffeine* (10 mM): polarity = 0.3 ± 0.1, speed = 4.1 ± 0.7 (n = 6), and; *Ionomycin* (14 μM): polarity = 1.8 ± 0.6, speed = 3.0 ± 0.6 (n = 6). Values mean ± standard error; speed was measured as micrometers per minute, polarity is dimensionless, and n indicates the number of cells. The control values reported are the mean speed and polarity for all cells for 45 s just prior to treatment.
10. R. A. Brundage and F. S. Fay, unpublished observations.
11. M. Scanlon, D. A. Williams, F. S. Fay, *J. Biol. Chem.* **13**, 6308 (1987).
12. The statistical significance of the differences in gradients of $[Ca^{2+}]_i$ in cells turning or moving straight ahead was determined using a paired comparison test. $[Ca^{2+}]_i$ gradients were divided into 20 equal segments for each cell. The average of three gradients points at the front of the cell was subtracted from the average of three gradient points at the rear of the cell for 16 images of cells moving straight ahead and 13 images of turning cells. To avoid possible edge effects, the last and first points of the gradient were not used. Unless indicated, all errors are given as the standard error of the mean.
13. M. Poenie, R. Y. Tsien, A. Schmidt-Verhulst, *EMBO J.* **6**, 2223 (1987).
14. M. Poenie, *Cell Calcium* **11**, 85 (1990).
15. Y. Wang, F. Lanni, P. L. McNeil, B. R. Ware, D. L. Taylor, *Proc. Natl. Acad. Sci. U.S.A.* **79**, 4660 (1982).
16. Measurements of $[Ca^{2+}]_i$ were compared with fluorescence anisotropy (r) of Fura-2 in the same cell or cellular region; $r = I_{\parallel} - I_{\perp}/I_{\parallel} + 2I_{\perp}$, was calculated from measurements of fluorescence at 510 nm, exciting with light at 360 nm polarized either parallel or perpendicular to an analyzer in the emission path. At the front and back of seven images of two cells, r averaged 0.213 ± 0.010 and 0.228 ± 0.003, respectively, while $[Ca^{2+}]$ was, on average, 13.0 ± 6.4 nM higher in the back in these same cells. Similar measurements of Fura-2 in Ca^{2+} buffers containing varying amounts of sucrose revealed that the gradient of anisotropy in the cell would tend to diminish the observed gradient of $[Ca^{2+}]_i$. Furthermore, no significant correlation was found between variations in whole cell $[Ca^{2+}]$ and r in these seven images (regression coefficient = −0.54; 95% confidence internal = −0.20 to +0.79). Differences in Fura-2 properties due to local differences in viscosity would be expected to produce detectable differences in r; for example, increasing sucrose from 1.5 to 2.0 M resulted in a decrease that would result in an underestimate of $[Ca^{2+}]_i$ by 16 nM and this was associated with an increase in r from 0.225 to 0.245 at 100 nM $[Ca^{2+}]$.
17. D. L. Taylor and M. Fechheiber, *Philos. Trans. R. Soc. London* **B299**, 185 (1982); S. J Smith, *Science* **242**, 708 (1988).
18. Y. Fukui, T. J. Lynch, H. Brzeska, E. D. Korn, *Nature* **341**, 328 (1989).
19. K. Collins, J. R. Sellers, P. Matsudara, *J. Cell Biol.* **110**, 1137 (1990).
20. D. Bray and J. G. White, *Science* **239**, 883 (1988).
21. N. M. McKenna, Y. Wang, M. E. Konkel, *J. Cell Biol.* **109**, 1163 (1989).
22. H. Yin and T. P. Stossel, *Nature* **281**, 583 (1979); T. P. Stossel *et al.*, *Annu. Rev. Cell Biol.* **1**, 353 (1985).
23. Y. L. Wang, *J. Cell Biol.* **101**, 597 (1985); S. J Smith, in (*17*); P. Forscher and S. J Smith, *J. Cell Biol.* **107**, 1505 (1988); L. Cassimeris, H. McNeill, S. H. Zigmond, *ibid.* **110**, 1067 (1990).
24. K. Kamm and J. T. Stull, *Annu. Rev. Pharmacol. Toxicol.* **25**, 593 (1985).
25. P. W. Marks, B. Hendey, F. R. Maxfield, *J. Cell Biol.* **112**, 149 (1991).
26. At each pixel, $[Ca^{2+}]_i$ was calculated from the ratio of fluorescence excited at 340:380 nm; the percentage of error associated with the $[Ca^{2+}]$ at each pixel was calculated from knowledge of the signal intensity and the sources of noise in the imaging system (*5*), and only pixels for which the percent error in the calculated $[Ca^{2+}]$ was less than or equal to 10% were retrieved for display or further analysis. The cells were pressure microinjected with Fura-2 to an intracellular concentration of approximately 100 μM for these studies.

27. Supported in part by NIH (HL14523) and NSF (DIR-8720188).

8 March 1991; accepted 25 June 1991